

AD-A116 452

AD A-116 452

TECHNICAL REPORT ARLCB-TR-82008

**TECHNICAL
LIBRARY**

SERVICE SIMULATION TESTS TO DETERMINE THE
FATIGUE LIFE OF OD NOTCHED THICK-WALL CYLINDERS

J. A. Kapp
J. H. Underwood

April 1982



US ARMY ARMAMENT RESEARCH AND DEVELOPMENT COMMAND
LARGE CALIBER WEAPON SYSTEMS LABORATORY
BENÉT WEAPONS LABORATORY
WATERVLIET, N. Y. 12189

AMCMS No. 6111.01.91A0.0

PRON No. 1A-1-2ZC36-0

APPROVED FOR PUBLIC RELEASE; DISTRIBUTION UNLIMITED

DISCLAIMER

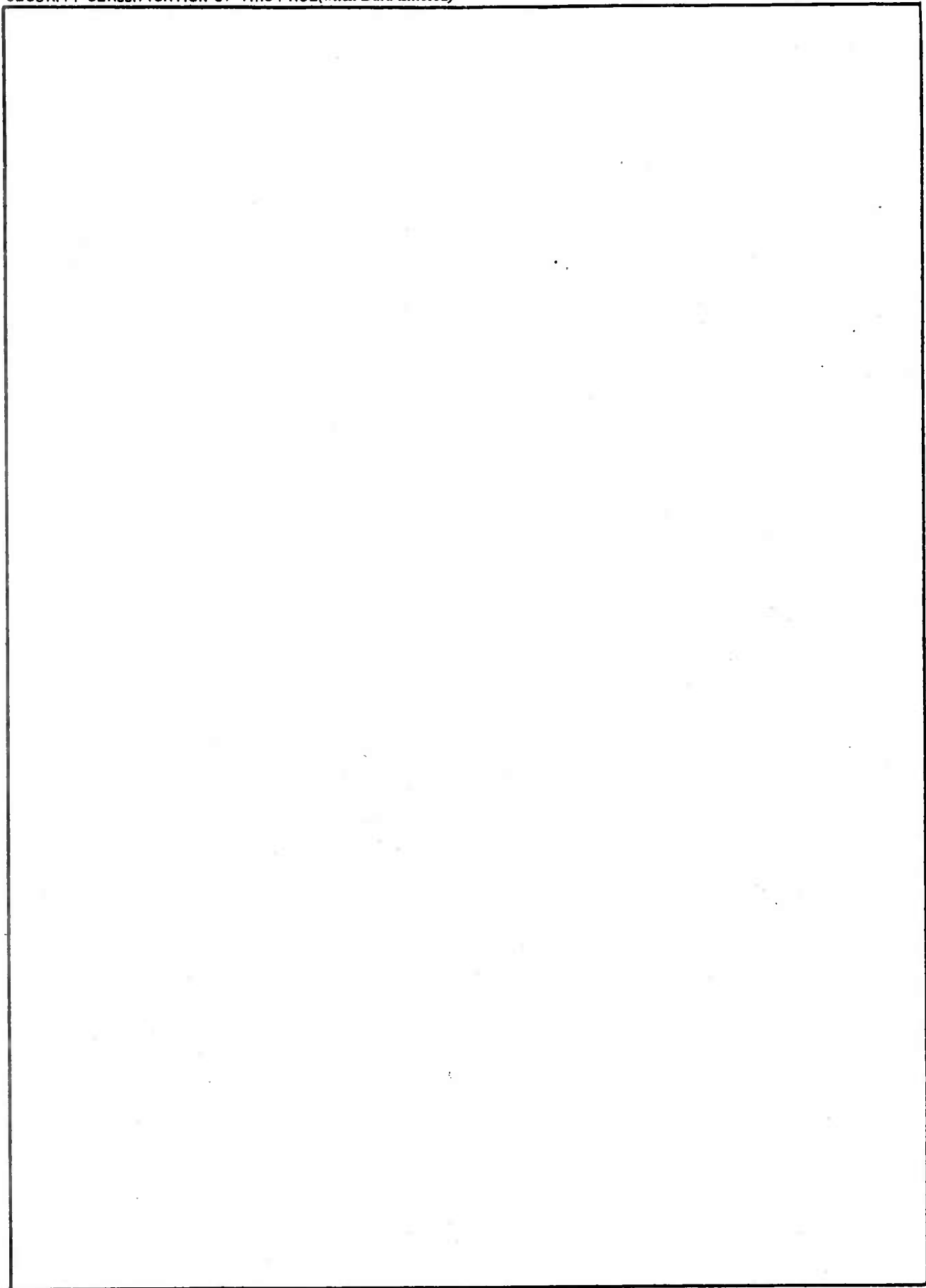
The findings in this report are not to be construed as an official Department of the Army position unless so designated by other authorized documents.

The use of trade name(s) and/or manufacture(s) does not constitute an official indorsement or approval.

DISPOSITION

Destroy this report when it is no longer needed. Do not return it to the originator.

SECURITY CLASSIFICATION OF THIS PAGE(When Data Entered)



SECURITY CLASSIFICATION OF THIS PAGE(When Data Entered)

TABLE OF CONTENTS

	<u>Page</u>
ACKNOWLEDGMENTS	iii
INTRODUCTION	1
THE OD NOTCHED CYLINDER PROBLEM	3
Simulation Specimen	5
Stresses for the Notched Cylinder	8
Stresses for Simulation Specimen	10
Loads for Simulation Specimens	16
TEST RESULTS	18
A Descriptive Model	20
CONCLUSIONS	22
REFERENCES	23

TABLES

I. STRESS CONCENTRATION FACTORS AND RESIDUAL STRESS RELIEF FACTORS FROM FINITE ELEMENT ANALYSIS	10
II. LOADS REQUIRED TO SIMULATE EFFECTS OF PRESSURE AND AUTOFRETTAGE	17
III. MEASURED FATIGUE LIFE OF PRESSURIZED CYLINDERS AND SIMULATION SPECIMENS	19
IV. FATIGUE LIFE CALCULATIONS	22

LIST OF ILLUSTRATIONS

1. Theoretical tangential stress distributions for a thick-walled autofrettaged cylinder with: $a = 77.5$ mm; $b = 135$ mm; $p = 386$ MPa; and $\sigma_{ys} = 1170$ MPa.	2
2. The OD notched cylinder.	4
3. The simulation specimen.	6

	<u>Page</u>
4a. The finite element mesh used.	11
4b. The refined grid.	12
5. Finite element results for the deep notch simulation specimen.	14
6. Finite element results for the shallow notch simulation specimen.	15

ACKNOWLEDGMENTS

The authors wish to acknowledge Mr. J. J. Zalinka for his careful execution of the experiments described here and Mr. D. P. Kendall for his assistance in the planning and analysis stages of the work.

INTRODUCTION

Residual stresses are often induced in thick-wall cylinders to increase the internal pressure which can be contained elastically and to enhance fatigue life upon cyclic pressurization. Several techniques are used to do this: shrink fitting of thick-wall jackets, wire wrapping, and autofrettage are examples.¹ The method used extensively in the manufacture of modern cannon is autofrettage. In this method the cylinder is subjected to an internal pressure sufficient to cause plastic deformation axisymmetrically to some radius ρ , the elastic-plastic radius. Upon removal of the autofrettage pressure, the cylinder recovers non-uniformly. Since the inner portion of the wall thickness is subjected to relatively large plastic strains, that portion of the cylinder will try to remain permanently deformed. The outer portions, being subjected to much smaller plastic strains or elastic strains, will attempt to recover to nearly their original positions. This results in a residual stress distribution which in the tangential direction is compressive at the inside diameter (ID) and varies logarithmically to tension through the plastically deformed region of the cylinder. Residual stresses also result in the radial and axial directions, but such stresses usually have little influence on the fatigue life of pressurized cylinders and are not considered here. Two theoretical autofrettage residual stress distributions (100% overstrain and 60% overstrain) are shown in Figure 1. Percent overstrain is that per-

¹Davidson, T. E. and Kendall, D. P., "The Design of High Pressure Containers and Associated Equipment," The Mechanical Behavior of Materials Under Pressure, Pugh, H.L.I.D., Ed., Elsevier Publishing, Amsterdam, 1970.

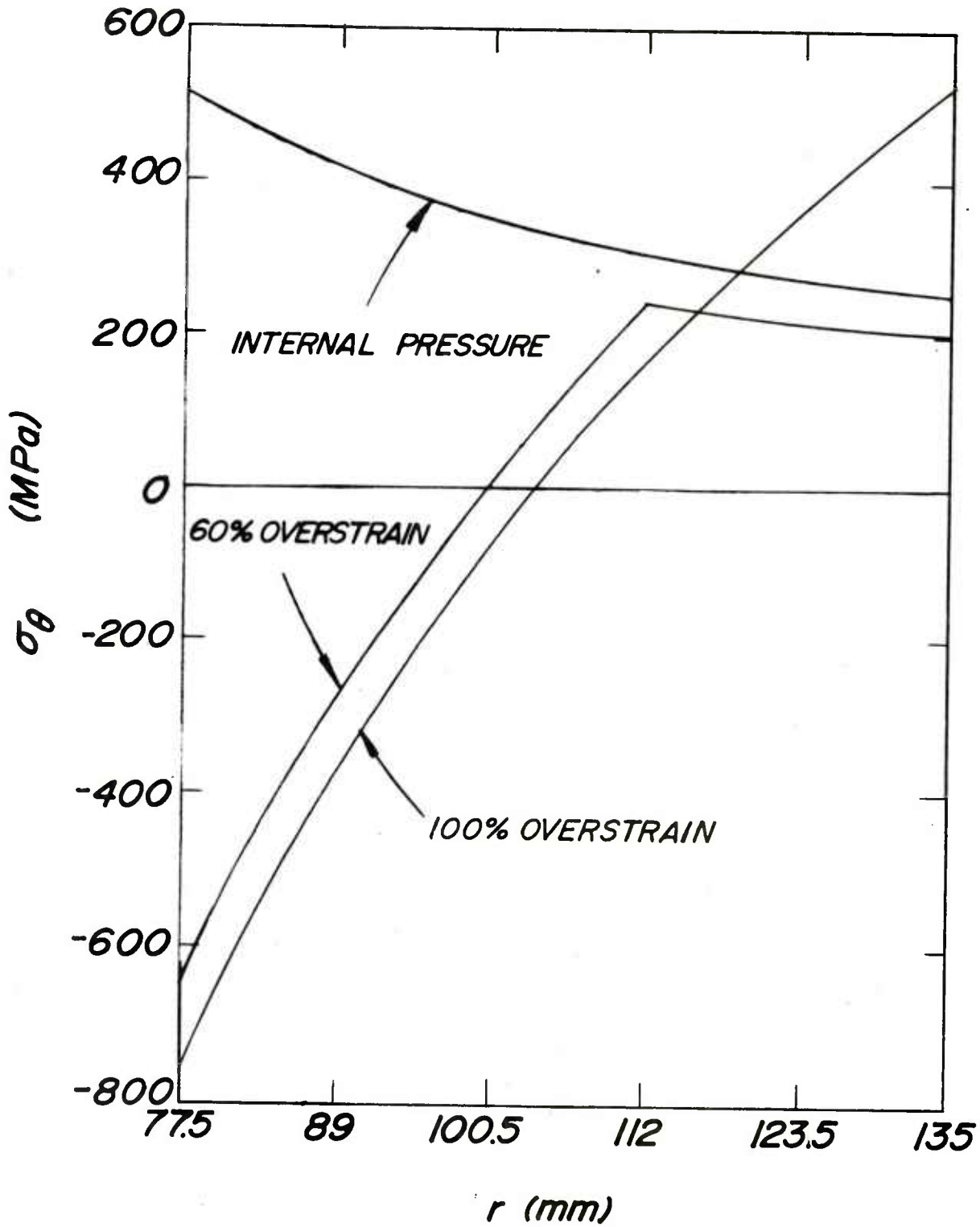


Figure 1. Theoretical Tangential Stress Distributions for a Thick-walled Autofrettaged Cylinder With $a=77.5$ mm; $b=135$ mm; $p= 386$ MPa; and $\sigma_{ys}=1170$ MPa.

centage of the wall thickness subjected to plastic deformation during the application of the autofrettage pressure.

It has been shown^{2,3} that autofrettage significantly increases the fatigue life of internally pressurized smooth cylinders in which the fatigue failure initiates at the ID. For some engineering applications it is necessary to introduce structural discontinuities such as holes and keyways at the outside diameter (OD) of cylinders. In these cylinders, the combination of tensile residual stress due to autofrettage, tensile operating stress due to internal pressure, and the stress concentration of the discontinuity causes fatigue crack initiation and growth at the OD, and fatigue life is reduced. The purpose of this paper is to determine the effects on fatigue life of reducing the amount of autofrettage residual stress and of reducing the depth of an OD notch.

THE OD NOTCHED CYLINDER PROBLEM

The cylinder of concern in this study is pictured in Figure 2. The dimensions of the cylinder are $a = 77.5$ mm, $b = 135$ mm, $h = 25$ mm, and $R = 1.5$ mm. The material is a Ni-Cr-Mo forged steel similar in composition to AISI 4335, heat treated to a nominal yield strength of 1170 MPa and ultimate strength of 1270 MPa. The cylinder was autofrettaged using 100 percent over-

²Davidson, T. E., Barton, C. S., Reiner, A. N., and Kendall, D. P., "Overstrain of High Strength Open End Cylinders of Intermediate Diameter Ratio," Proceedings of the First International Congress on Experimental Mechanics, Pergamon Press, Oxford, 1963.

³Davidson, T. E. and Throop, J. F., Practical Fracture Mechanics Applications to Design of High Pressure Vessels, John J. Burke and Volker Weiss, Eds., Plenum Press, 1979.

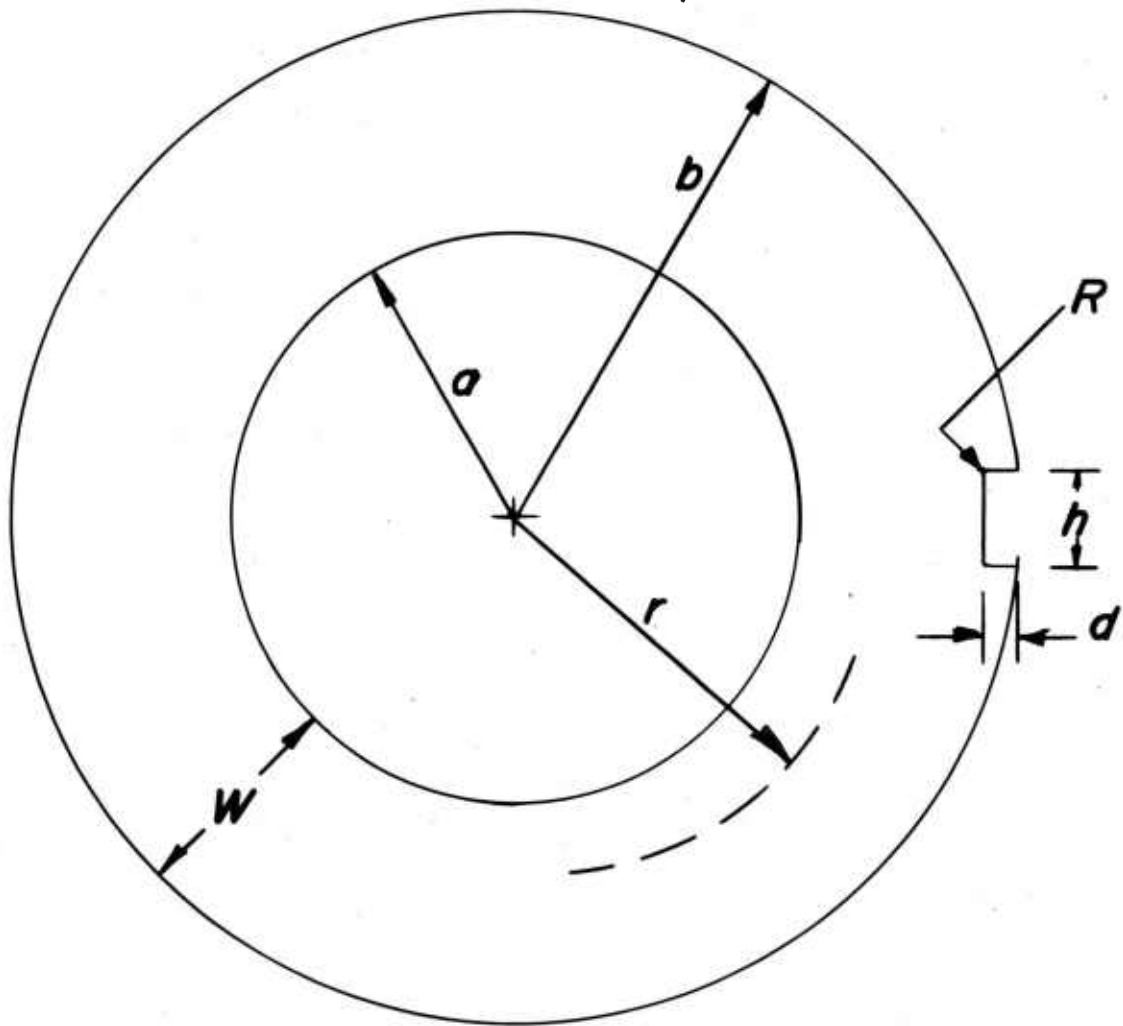


Figure 2. The OD Notched Cylinder

strain, that is, 100 percent of the wall thickness was subjected to plastic deformation during the application of the autofrettage pressure. The OD notch is introduced after the cylinder has been autofrettaged. When such cylinders 2m long were subjected to 0 to 386 MPa pressure cycles, fatigue failure occurred at the root of the notch at a relatively short life compared to un-notched cylinders. The failure occurred by initiation and growth of small surface cracks over nearly the entire axial length of the notch. Complete through-wall fracture occurred soon after these small cracks combined to form a long, shallow-depth, straight-fronted crack. The study here was undertaken to simulate this fatigue behavior with a simple, inexpensive specimen. This specimen is used to determine the effect on fatigue life of reducing the percent overstrain and the associated tensile residual stress at the OD and to determine the effect on life of reducing the depth, d , of the notch.

Simulation Specimen

There are a number of important features which a simulation specimen must have in order to obtain a good approximation of fatigue behavior. Similar materials, geometry, and stresses are three general features which are particularly important. In the tests here, the simulation specimens were taken from one of the cylinders of concern, so the material is well simulated. Regarding geometry and stresses, if either one is simulated well enough, this should suffice. But this is seldom possible or practical, so the approach usually taken is to simulate both geometry and stresses as closely as possible at the location of expected failure. The simulation specimen used here is shown in Figure 3. Specimens with $d = 10$ mm and $d = 5$ mm were tested; in both cases h and R are the same. The cross-section geometry at the notch, where fatigue

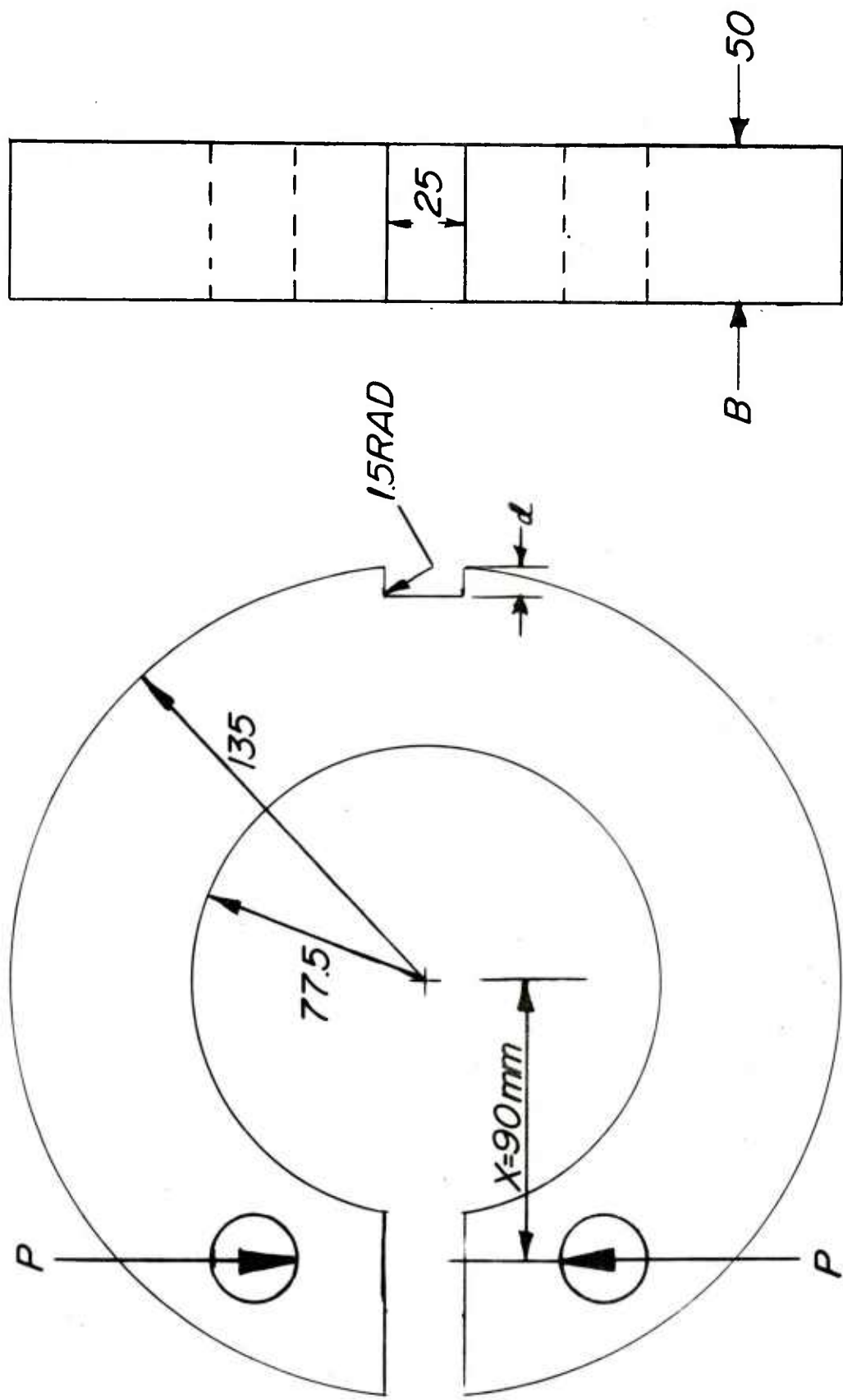


Figure 3. The Simulation Specimen.

failure occurs, is made the same as the cylinder; the geometry opposite the notch is different, and the dimension of the simulation specimen along the axis is quite different, that is, 50 mm compared with 2m for the cylinder. The stresses at the notch are the only stresses which need to be closely simulated in the specimen. This is all that is necessary because once the small cracks at the cylinder notch combine and begin to grow into the wall, failure is imminent. If the cylinder were capable of tolerating large amounts of stable crack growth prior to complete fracture, it would also have been necessary to simulate the thru-thickness stress distributions in addition to the conditions at the root of the notch.

Since the stresses in the vicinity of the notch in the cylinder are tensile, as shown in Figure 1, tensile stresses are required near the notch in the simulation specimen. This is accomplished by applying compressive loads through pin holes, as indicated in Figure 3. On the radial plane intersecting the root of the notch, the total stress resulting from the compressive load is a compressive normal stress plus a bending stress which varies from compression at the ID to tension at the OD. The specimen is designed such that the tensile bending stress at the OD is far greater than the compressive normal stress, so the resultant is tensile in the vicinity of the notch. The stresses resulting in the simulation specimen were determined using an approximate linear bending analyses and using a finite element analysis which accounted for the specific notch geometry. These results are given in the upcoming section.

Stresses for the Notched Cylinder

The stresses at the cylinder notch which are to be simulated in the specimen are a minimum stress corresponding to the tensile autofrettage residual stress and a stress range resulting from the cyclic internal pressure in the cylinder. The residual stress in the tangential direction due to autofrettage, $\sigma_{\theta a}$, calculated assuming the Tresca yield criterion, rigid plastic material behavior, and plane strain conditions, is given as:²

$$\frac{\sigma_{\theta a}}{\sigma_{ys}} = \begin{cases} \frac{a^2}{b^2-a^2} \left(1 + \frac{b^2}{r^2}\right) \left(\frac{\rho^2-b^2}{2b^2} - \ln \frac{\rho}{a}\right) + \left(\frac{\rho^2+b^2}{2b^2} - \ln \frac{\rho}{r}\right) & a < r < \rho \\ \left(1 + \frac{b^2}{r^2}\right) \left(\frac{\rho^2}{2b^2} + \frac{a^2}{b^2-a^2} \left(\frac{\rho^2-b^2}{2b^2} - \ln \frac{\rho}{a}\right)\right) & \rho < r < b \end{cases} \quad (1)$$

in which σ_{ys} is the uniaxial yield strength, ρ is the elastic-plastic radius, and other quantities as in Figure 2. Plots of Eq. (1) for two values of ρ are shown in Figure 1. The tangential stress, $\sigma_{\theta p}$ resulting from the internal pressure, p , in the cylinder follows the well known Lamé' solution:

$$\sigma_{\theta p} = \frac{pa^2}{b^2-a^2} \left(1 + \frac{b^2}{r^2}\right) \quad (2)$$

The tangential stress is the only stress considered because it is the maximum principal tensile stress and thus it controls fatigue crack growth.

²Davidson, T. E., Barton, C. S., Reiner, A. N., and Kendall, D. P., "Overstrain of High Strength Open End Cylinders of Intermediate Diameter Ratio," Proceedings of the First International Congress on Experimental Mechanics, Pergamon Press, Oxford, 1963.

The presence of the notch on the OD will significantly modify the theoretical stress distributions of equations (1) and (2). Finite element solutions for this problem have been developed recently by Kapp and Pflegl.⁴ These results show that a notch produces a significant stress concentration factor, K_t , under either internal pressure or residual stress loading. The finite element results also show that a notch substantially relieves the autofrettage residual stresses throughout the cylinder. Using these results, the stresses to be produced at the notch ($r=b-d$) in our simulation specimens are:

$$\sigma_{Na} = K_{ta}R_f[\sigma_{\theta a}(r=b-d)] \quad (3)$$

$$\sigma_{Np} = K_{tp}[\sigma_{\theta p}(r=b-d)] \quad (4)$$

The stresses σ_{Na} and σ_{Np} are respectively the notch stresses due to autofrettage and pressure loading, R_f is a factor which indicates the extent to which the overall level of residual stress in the cylinder is relieved by the notch, and $\sigma_{\theta a}$ and $\sigma_{\theta p}$ are given by equations (1) and (2). Stress concentration factors and R_f factors for two notch depths and three loading conditions are given in Table I from the results in Reference 4. The values of K_t are the ratio of the maximum stress at the root of the notch ($r=b-d$) to the stress predicted at the same radial position using equation (1) or (2). The values of R_f are ratios of the tangential stress in the notched cylinder (180° away from the notch) to that in the unnotched cylinder.

⁴Kapp, J. A. and Pflegl, G. A., "Stress Analysis of OD Notched Thick-Walled Cylinders Subjected to Internal Pressure or Thermal Loads," J. Pressure Vessel Technology, Vol. 103, 1981, pp. 76-89.

TABLE I. STRESS CONCENTRATION FACTORS AND RESIDUAL STRESS RELIEF FACTORS FROM FINITE ELEMENT ANALYSIS

Deep Notch d = 10 mm	Pressurized Cylinder	60% Overstrained Cylinder	100% Overstrained Cylinder
K_t	5.4	5.8	6.6
R_f	1	0.71	0.70
Shallow Notch d = 5 mm			
K_t	3.5	3.5	3.7
R_f	1	0.72	0.70

Stresses for Simulation Specimens

The stresses produced in the simulation specimen were determined using finite element analysis. Figure 4(a) shows the finite element mesh used to analyze the shallow notch geometry (d = 5 mm), indicating the boundary and loading conditions. Since the specimen is symmetric about the plane bisecting the notch, only one half of the specimen need be analyzed to determine the stresses. The elements used were constant strain triangles and quadrilateral two dimensional plate elements. The analysis was conducted using the NASTRAN computer program⁵ on an IBM 360/44. To determine the stresses at the root of the notch it was necessary to refine the finite element mesh around the root radius R. The mesh shown in Figure 4(b) was used to do this.

⁵McCormick, C. W., "NASTRAN User's Manual," The MacNeal-Schwendler Corp., 1969.

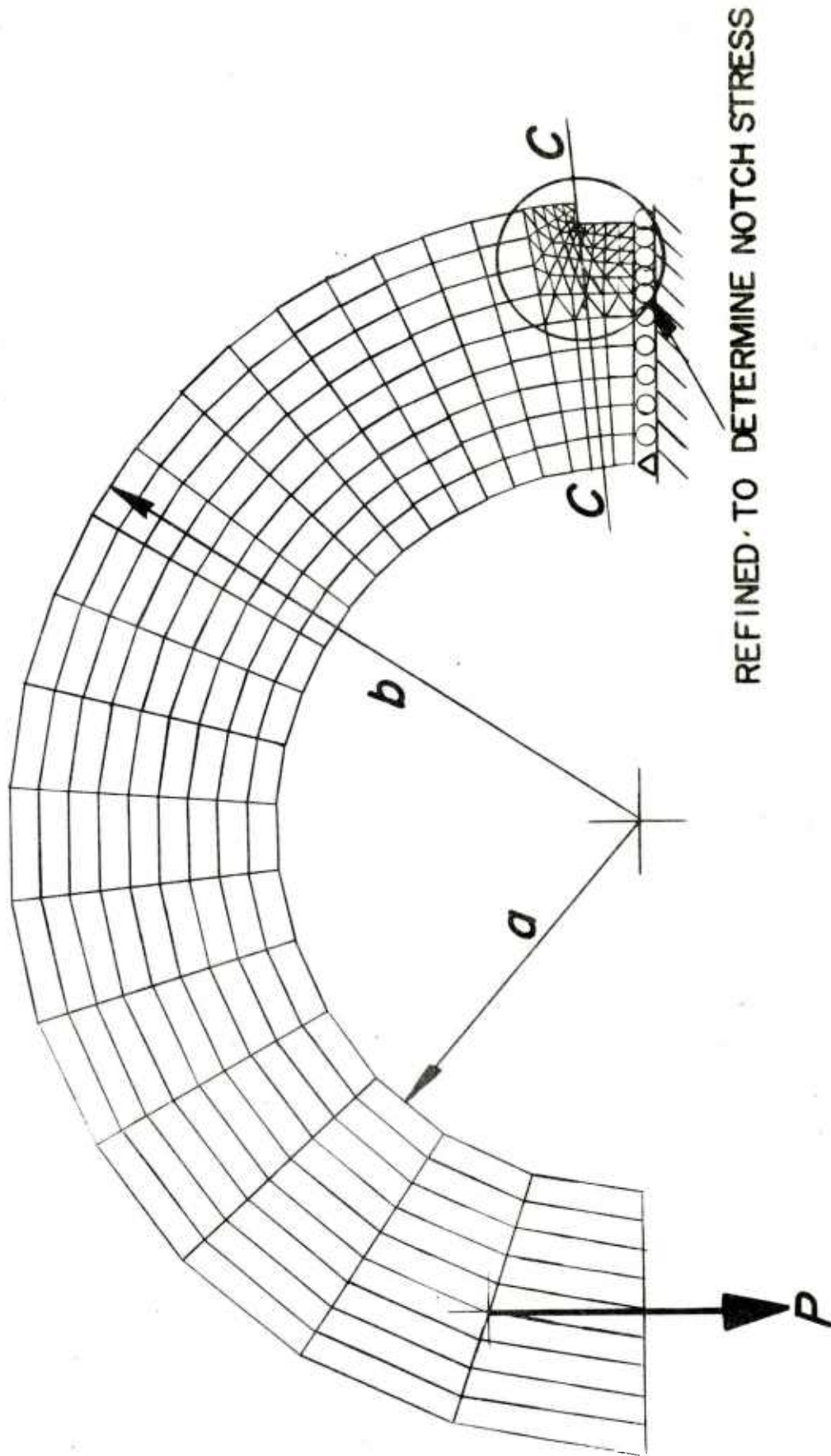


Figure 4a. The Finite Element Mesh Used

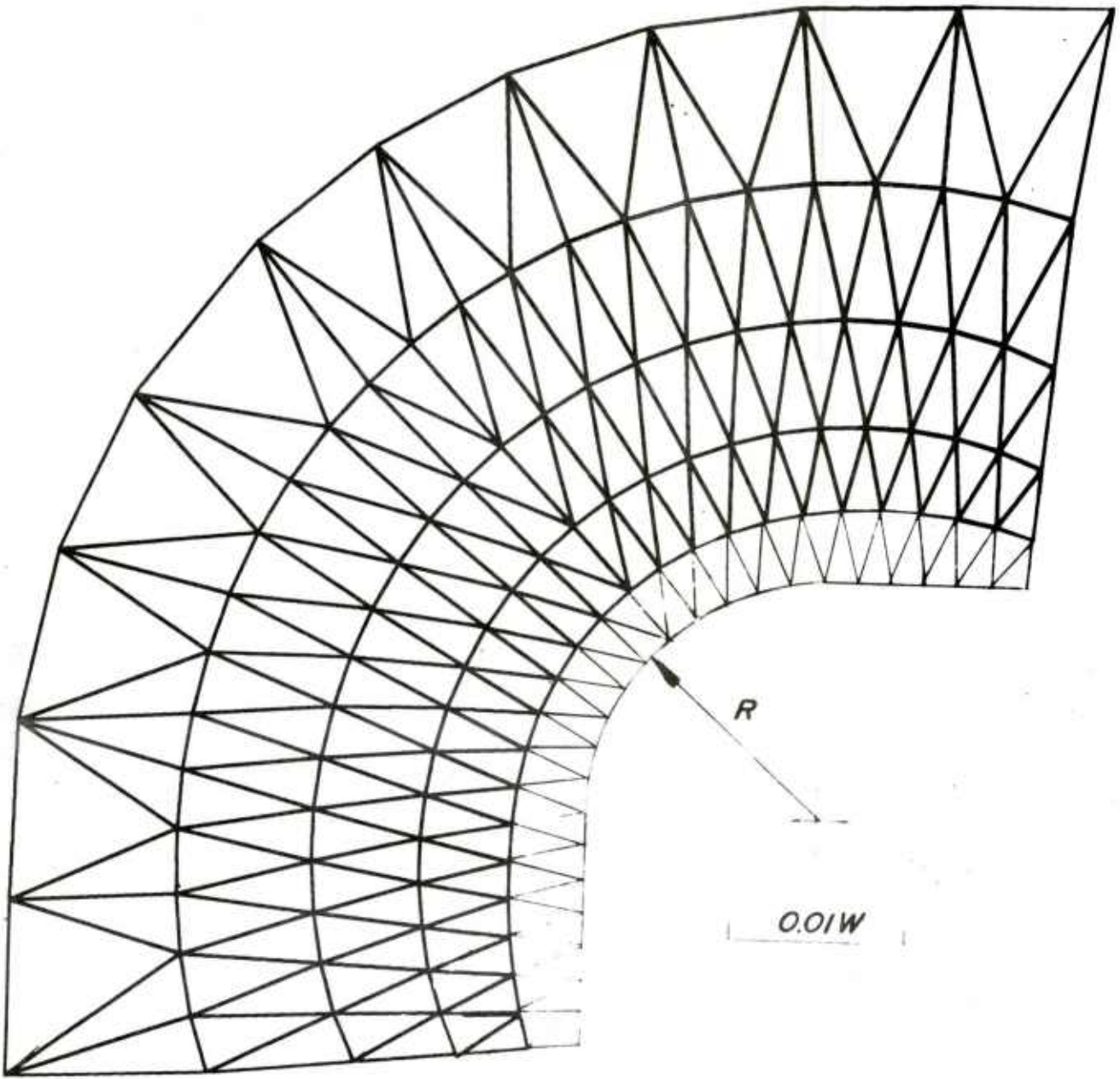


Figure 4b. The refined Grid

The finite element solutions for the simulation specimens appear in Figures 5 and 6. The data points are the stresses along plane C-C, the radial plane which intersects the root of the notch. For comparison, an approximate solution based on linear bending theory is shown in Figures 5 and 6. Prior work⁶ in similar specimen geometries has shown that linear bending is a good approximation. This linear bending solution is the sum of the normal and bending stresses in the full wall thickness assuming that the notch is not present. The sum of the stresses is:

$$\sigma = \frac{-P}{BW} + \left[\frac{6P(x+a+W/2)}{BW^2} \right] \left[\frac{2(r-a)}{W} - 1 \right] \quad (5)$$

where $-P/BW$ is the compressive normal stress, the first bracketed term is the bending stress, and the second bracketed term describes the linear variation of the bending stress with r . The stresses from the finite element solutions are significantly greater than the approximate solution, equation (5) at locations near the notch. This is expected because of the stress concentration of the notch.

⁶Kapp, J. A., Newman, J. C. Jr., and Underwood, J. H., "A Wide Range Stress Intensity Factor Expression For the C-Shaped Specimen," J. of Testing and Evaluation, Vol. 8, No. 6, Nov. 1980, pp. 314-317.

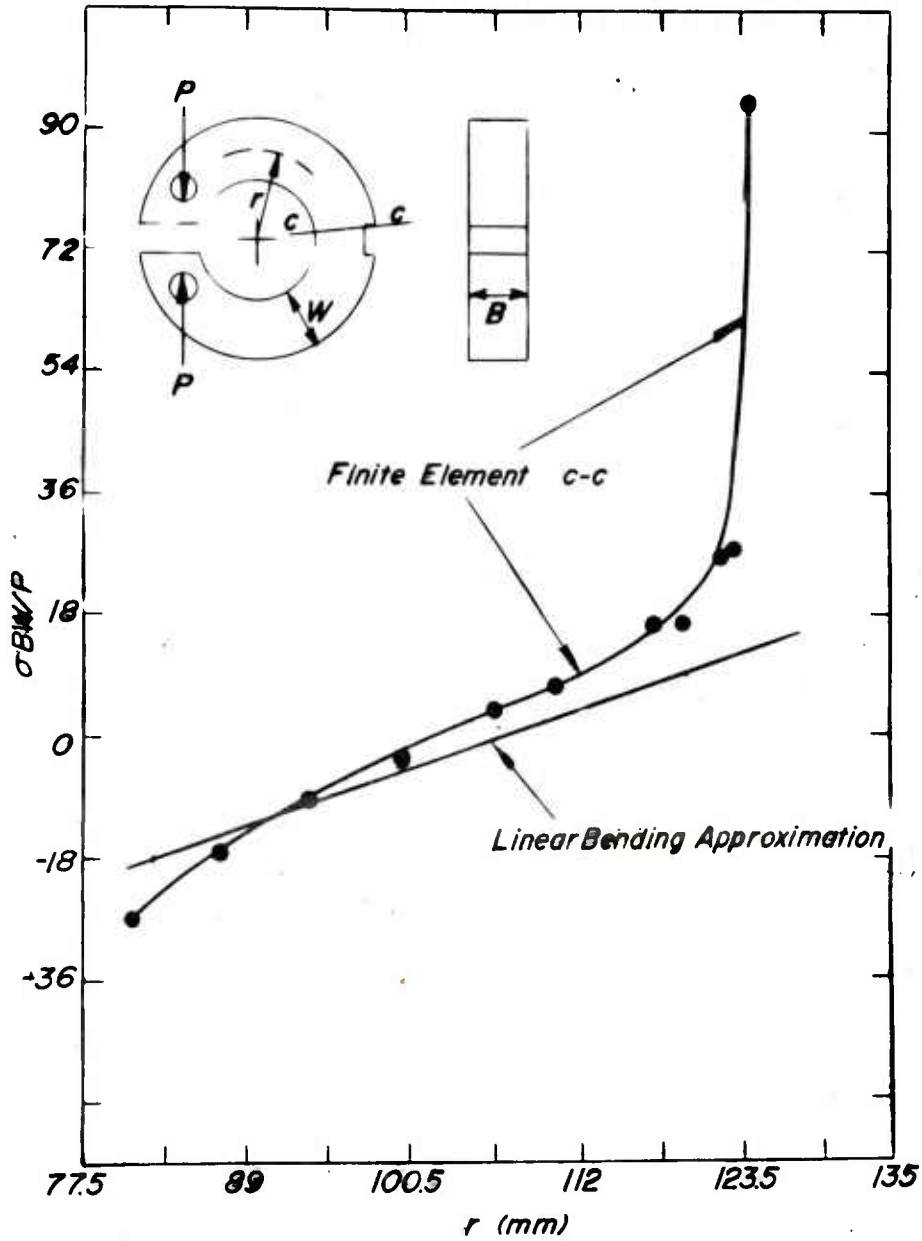


Figure 5. Finite Element Results for The Deep Notch Simulation Specimen

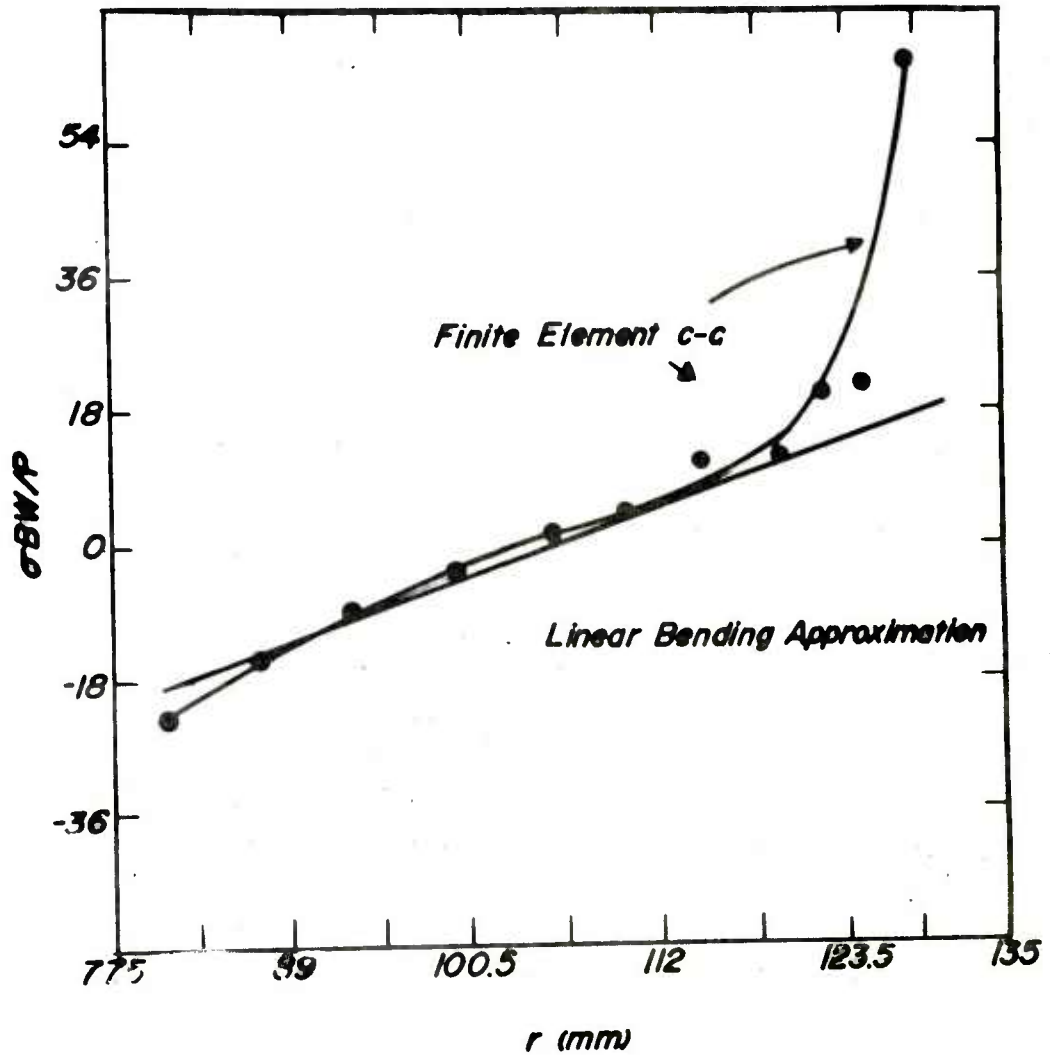


Figure 6. Finite Element Results for The Shallow Notch Simulation Specimen

Loads for Simulation Specimens

The results from Figures 5 and 6 show that the notch is a significant stress riser in the simulation specimen near the notch root. As previously mentioned, the actual stress distribution through the wall thickness is not important; only the stresses near the root of the notch are necessary for an adequate simulation of service conditions. Bearing this in mind, the following equations were developed to calculate loads necessary to simulate service conditions. For the deep notch:

$$\sigma_N = 89.2 \frac{P}{BW} \quad (6)$$

and for the shallow notch:

$$\sigma_N = 56.0 \frac{P}{BW} \quad (7)$$

where P is the applied load, B and W are the specimen dimensions shown in Figure 3. The constant coefficients were determined from Figures 5 and 6 at r values corresponding to the deep and shallow notches, respectively. A simulation of service conditions would be accomplished when, for a deep notch for example, equation (6), is equated with the sum of equations (3) and (4) and P is solved for. This was done for the loading conditions and the notch configurations studied here. Table II summarizes the results of these calculations; P_{max} is the load which simulates the combination of pressure and autofrettage loading, and P_{min} is the load which simulates just autofrettage loading.

Since the finite element solutions were not available at the time of the testing, the simulation loads were determined using equations (1), (2), and (5). The criterion used in the calculation was that the stresses acting at the radial position r=b-d should be the same in the simulation specimen using

equation (5), and in the cylinder using equations (1) and (2). This assumes that the notch will concentrate the stresses in the simulation specimen the same way they are concentrated in the cylinder. Specifically, the minimum load P_{min} was determined by equating equation (1) with equation (5), both with $r=b-d$, and the maximum load P_{max} was determined using the same approach with equations (2) and (5), and adding this load to P_{min} . This was done for both the deep notch ($d = 10$ mm) and for the shallow notch ($d = 5$ mm). The difference between the calculations for deep and shallow notches is small, so the same nominal loads were used for both notch configurations. These loads are shown in Table II.

TABLE II. LOADS REQUIRED TO SIMULATE EFFECTS OF PRESSURE AND AUTOFRETTAGE

Notch Depth mm	Autofrettage Overstrain %	Loads Based on Notch Stress; Eqs. 3,4,6,7 kN	Loads Used in Tests kN
10	100	P_{max} : 138	175
		P_{min} : 68	95
10	60	P_{max} : 103	132
		P_{min} : 33	52
5	100	P_{max} : 119	175
		P_{min} : 50	95
5	60	P_{max} : 100	132
		P_{min} : 31	52

TEST RESULTS

The measured fatigue lives to compute failure of the simulation specimens under the different loading conditions are presented in Table III along with prior results from two pressurized cylinders. In all cases the fracture of the simulation specimen occurred very soon after a straight crack was initiated across the depth, B, of specimen at the root of the notch, which is the same mode of failure observed in testing of pressurized cylinders. So in this respect, the tests were a close approximation to the behavior which occurred in service.

The results from the control specimens, D2 and D3 are in good agreement with the fatigue results obtained from pressurized cylinders. The difference in average measured life between the cylinder tests and the control specimens is about 10% and is less than the scatter in either set of data. The results from the testing of the other conditions show that by either decreasing the amount of autofrettage overstrain or decreasing the notch depth, a significant increase in fatigue life is obtained. These results are expected since by decreasing the amount of overstrain, the minimum stress occurring during the fatigue cycle is reduced, which means that the mean stress is reduced, and it is well known that reductions in mean stress result in increased fatigue life. By decreasing the notch depth, the stress concentration factor is decreased, as is verified by the finite element results. This also is known to result in increased fatigue life.

TABLE III. MEASURED FATIGUE LIFE OF PRESSURIZED CYLINDERS
AND SIMULATION SPECIMENS

	Notch Depth mm	Overstrain %	Life to Failure cycles	Average Life cycles
<u>Pressurized Cylinders:</u>				
#22684	10	100	2752	3020
#22537	10	100	3288	
<u>Simulation Specimen:</u>				
D2	10	100	3003	2728
D3	10	100	2452	
D4	10	60	4079	4166
D5	10	60	4252	
S1	5	100	9280	10,252
S2	5	100	11,224	
S3	5	60	42,985	41,626
S4	5	60	40,266	

The test results in Table III can be used to determine which of the two key variables, that is, mean stress or stress concentration factor, has the most effect on fatigue life. Separate comparisons of the deep and shallow notch test results show a factor of 1.5 increase in fatigue life for the deep notch tests due to the decrease in overstrain and thus mean stress, and a factor of 4.1 increase in fatigue life for the shallow notch tests due to the

decrease in notch depth and thus stress concentration factor. So it is clear that for the tests here the notch depth and associated stress concentration factor has a more significant effect on fatigue life than does mean stress as controlled by autofrettage overstrain.

A Descriptive Model

To describe the type of behavior observed in the tests, a model that accounts for both mean stress effects and stress concentration effects may be useful. Such a model has been proposed by Fuchs.⁷ His model states that fatigue crack initiation will occur when the following condition is obtained:

$$\sigma_e < \frac{K_f}{\sqrt{2}} \left(\frac{\Delta\sigma}{2} + C\sigma_m \right) \quad (8)$$

where σ_e is the endurance limit of the material, $\Delta\sigma$ and σ_m are the nominal stress range and mean stress of the fatigue cycle, C is a material constant, and K_f is the fatigue stress concentration factor. Equation (8) was first proposed as a condition for fatigue crack initiation at long life, $> 10^6$ cycles, but it may be useful for describing the fatigue life behavior of the tests here. Even though the lives here are somewhat below 10^6 cycles, they are primarily initiation controlled.

No S-N tests and analyses were performed for the material here, so direct life predictions can not be made with Equation (8). However, the effects of the test variables can be estimated by using the following approach based on Equation (8).

⁷Fuchs, H. D., Trans. ASME, Ser. D., J. Basic Eng., Vol. 87, 1965, pp. 333-343.

$$N_f = \left[\frac{\text{constant}}{K_t (\Delta\sigma + \sigma_m)} \right]^3 \quad (9)$$

Equation (9) states that fatigue life varies inversely with the third power of an effective stress which is represented by similar parameters as those in Fuch's model, that is, stress concentration factor, stress range and mean stress. Table IV lists nominal values of these parameters from the results here and the calculated values of N_f from Equation (9). The constant in Equation (9) was set at the value such that the calculated and measured lives are the same for the control condition, that is, for the deep notch and 100% overstrain. The power 3 in the equation was based on recent experience⁸ in which the third power of stress gave a good representation of fatigue life of notched components.

Considering the difficulties and the scatter in fatigue life testing and the uncertainties in fatigue life calculations, the agreement between calculated and actual lives in Table IV is considered to be good. Therefore, this approach for calculating fatigue lives based on Fuch's model is believed to be generally applicable for describing results from tests which involve notched geometries and variations in mean and alternating stresses.

⁸Underwood, J. H. and Kapp, J. A., "Benefits of Overload for Fatigue Cracking at a Notch," Fracture Mechanics: Thirteenth Conference, ASTM STP 743, Richard Roberts, Ed., American Society for Testing and Materials, 1981, to be published.

TABLE IV. FATIGUE LIFE CALCULATIONS

Overstrain %	$\Delta\sigma = \sigma_{\theta p}$ MPa	$\sigma_m = R_f \cdot \sigma_{\theta a}$ MPa	K_t	Calculated Life cycles	Measured Life cycles
<u>Deep Notch:</u>					
100	404	481	6.0	2730	2730
60	404	362	6.0	4209	4170
<u>Shallow Notch:</u>					
100	388	527	3.6	11,443	10,250
60	388	347	3.6	22,068	41,630

CONCLUSIONS

The fatigue behavior of an OD notched internally pressurized cylinder can be modeled and simulated very well and inexpensively using ring specimens with the same OD notch and loaded in compression in a fatigue machine. Such specimens then can be used to determine the effects on fatigue life of reducing the notch depth and reducing the amount of autofrettage residual tension stress. Both of these changes will result in increased fatigue life. The test results and calculations based on a model similar to Fuch's⁷ show that notch depth has a more significant effect on life than does residual stress.

⁷Fuchs, H. D., Trans. ASME, Ser. D., J. Basic Eng., Vol. 87, 1965, pp. 333-343.

REFERENCES

1. Davidson, T. E. and Kendall, D. P., "The Design of High Pressure Containers and Associated Equipment," The Mechanical Behavior of Materials Under Pressure, Pugh, H.L.I.D., Ed., Elsevier Publishing, Amsterdam, 1970.
2. Davidson, T. E., Barton, C. S., Reiner, A. N.; and Kendall, D. P., "Overstrain of High Strength Open End Cylinders of Intermediate Diameter Ratio," Proceedings of the First International Congress on Experimental Mechanics, Pergamon Press, Oxford, 1963.
3. Davidson, T. E. and Throop, J. F., Practical Fracture Mechanics Applications to Design of High Pressure Vessels, John J. Burke and Volker Weiss, Eds., Plenum Press, 1979.
4. Kapp, J. A. and Pflagl, G. A., "Stress Analysis of OD Notched Thick-Walled Cylinders Subjected to Internal Pressure or Thermal Loads," J. Pressure Vessel Technology, Vol. 103, 1981, pp. 76-89.
5. McCormick, C. W., "NASTRAN User's Manual," The MacNeal-Schwendler Corp., 1969.
6. Kapp, J. A., Newman, J. C. Jr, and Underwood, J. H., "A Wide Range Stress Intensity Factor Expression For the C-Shaped Specimen," J. of Testing and Evaluation, Vol. 8, No. 6, Nov. 1980, pp. 314-317.
7. Fuchs, H. D., Trans. ASME, Ser. D., J. Basic Eng., Vol. 87, 1965, pp. 333-343.
8. Underwood, J. H. and Kapp, J. A., "Benefits of Overload for Fatigue Cracking at a Notch," Fracture Mechanics: Thirteenth Conference, ASTM STP 743, Richard Roberts, Ed., American Society for Testing and Materials, 1981, to be published.

TECHNICAL REPORT EXTERNAL DISTRIBUTION LIST

	<u>NO. OF COPIES</u>		<u>NO. OF COPIES</u>
ASST SEC OF THE ARMY RESEARCH & DEVELOPMENT ATTN: DEP FOR SCI & TECH THE PENTAGON WASHINGTON, D.C. 20315	1	COMMANDER US ARMY TANK-AUTMV R&D COMD ATTN: TECH LIB - DRDTA-UL MAT LAB - DRDTA-RK WARREN, MICHIGAN 48090	1 1
COMMANDER US ARMY MAT DEV & READ. COMD ATTN: DRCDE 5001 EISENHOWER AVE ALEXANDRIA, VA 22333	1	COMMANDER US MILITARY ACADEMY ATTN: CHMN, MECH ENGR DEPT WEST POINT, NY 10996	1
COMMANDER US ARMY ARRADCOM ATTN: DRDAR-LC -LCA (PLASTICS TECH EVAL CEN) -LCE -LCM -LCS -LCW -TSS (STINFO) DOVER, NJ 07801	1 1 1 1 1 2	US ARMY MISSILE COMD REDSTONE SCIENTIFIC INFO CEN ATTN: DOCUMENTS SECT, BLDG 4484 REDSTONE ARSENAL, AL 35898 COMMANDER REDSTONE ARSENAL ATTN: DRSMI-RRS -RSM ALABAMA 35809	2 1 1
COMMANDER US ARMY ARRCOM ATTN: DRSAR-LEP-L ROCK ISLAND ARSENAL ROCK ISLAND, IL 61299	1	COMMANDER ROCK ISLAND ARSENAL ATTN: SARRI-ENM (MAT SCI DIV) ROCK ISLAND, IL 61299	1
DIRECTOR US ARMY BALLISTIC RESEARCH LABORATORY ATTN: DRDAR-TSB-S (STINFO) ABERDEEN PROVING GROUND, MD 21005	1	COMMANDER HQ, US ARMY AVN SCH ATTN: OFC OF THE LIBRARIAN FT RUCKER, ALABAMA 36362	1
COMMANDER US ARMY ELECTRONICS COMD ATTN: TECH LIB FT MONMOUTH, NJ 07703	1	COMMANDER US ARMY FGN SCIENCE & TECH CEN ATTN: DRXST-SD 220 7TH STREET, N.E. CHARLOTTESVILLE, VA 22901	1
COMMANDER US ARMY MOBILITY EQUIP R&D COMD ATTN: TECH LIB FT BELVOIR, VA 22060	1	COMMANDER US ARMY MATERIALS & MECHANICS RESEARCH CENTER ATTN: TECH LIB - DRXMR-PL WATERTOWN, MASS 02172	2

NOTE: PLEASE NOTIFY COMMANDER, ARRADCOM, ATTN: BENET WEAPONS LABORATORY, DRDAR-LCB-TL, WATERVLIET ARSENAL, WATERVLIET, N.Y. 12189, OF ANY REQUIRED CHANGES.

TECHNICAL REPORT EXTERNAL DISTRIBUTION LIST (CONT.)

	<u>NO. OF COPIES</u>		<u>NO. OF COPIES</u>
COMMANDER US ARMY RESEARCH OFFICE P.O. BOX 12211 RESEARCH TRIANGLE PARK, NC 27709	1	COMMANDER DEFENSE TECHNICAL INFO CENTER ATTN: DTIA-TCA CAMERON STATION ALEXANDRIA, VA 22314	12 (2-LTD)
COMMANDER US ARMY HARRY DIAMOND LAB ATTN: TECH LIB 2800 POWDER MILL ROAD ADELPHIA, MD 20783	1	METALS & CERAMICS INFO CEN BATTELLE COLUMBUS LAB 505 KING AVE COLUMBUS, OHIO 43201	1
DIRECTOR US ARMY INDUSTRIAL BASE ENG ACT ATTN: DRXPE-MT ROCK ISLAND, IL 61299	1	MECHANICAL PROPERTIES DATA CTR BATTELLE COLUMBUS LAB 505 KING AVE COLUMBUS, OHIO 43201	1
CHIEF, MATERIALS BRANCH US ARMY R&S GROUP, EUR BOX 65, FPO N.Y. 09510	1	MATERIEL SYSTEMS ANALYSIS ACTV ATTN: DRXSY-MP ABERDEEN PROVING GROUND MARYLAND 21005	1
COMMANDER NAVAL SURFACE WEAPONS CEN ATTN: CHIEF, MAT SCIENCE DIV DAHLGREN, VA 22448	1		
DIRECTOR US NAVAL RESEARCH LAB ATTN: DIR, MECH DIV CODE 26-27 (DOC LIB) WASHINGTON, D.C. 20375	1 1		
NASA SCIENTIFIC & TECH INFO FAC P.O. BOX 8757, ATTN: ACQ BR BALTIMORE/WASHINGTON INTL AIRPORT MARYLAND 21240	1		

NOTE: PLEASE NOTIFY COMMANDER, ARRADCOM, ATTN: BENET WEAPONS LABORATORY,
DRDAR-LCB-TL, WATERVLIET ARSENAL, WATERVLIET, N.Y. 12189, OF ANY
REQUIRED CHANGES.

TECHNICAL REPORT INTERNAL DISTRIBUTION LIST

	<u>NO. OF COPIES</u>
COMMANDER	1
CHIEF, DEVELOPMENT ENGINEERING BRANCH	1
ATTN: DRDAR-LCB-DA	1
-DM	1
-DP	1
-DR	1
-DS (SYSTEMS)	1
-DS (ICAS GROUP)	1
-DC	1
CHIEF, ENGINEERING SUPPORT BRANCH	1
ATTN: DRDAR-LCB-SE	1
-SA	1
CHIEF, RESEARCH BRANCH	2
ATTN: DRDAR-LCB-RA	1
-RC	1
-RM	1
-RP	1
TECHNICAL LIBRARY	5
ATTN: DRDAR-LCB-TL	
TECHNICAL PUBLICATIONS & EDITING UNIT	2
ATTN: DRDAR-LCB-TL	
DIRECTOR, OPERATIONS DIRECTORATE	1
DIRECTOR, PROCUREMENT DIRECTORATE	1
DIRECTOR, PRODUCT ASSURANCE DIRECTORATE	1

NOTE: PLEASE NOTIFY DIRECTOR, BENET WEAPONS LABORATORY, ATTN: DRDAR-LCB-TL,
OF ANY REQUIRED CHANGES.